ACS APPLIED MATERIALS & INTERFACES

Research Article

www.acsami.org

Highly Bendable, Conductive, and Transparent Film by an Enhanced Adhesion of Silver Nanowires

Yang Li, Peng Cui, Luyang Wang, Hanleem Lee, Keunsik Lee, and Hyoyoung Lee*

National Creative Research Initiative, Centre for Smart Molecular Memory, Department of Chemistry and Department of Energy Science, Sungkyunkwan University, 300 Cheoncheon-Dong, Jangan-Gu, Suwon, Gyeonggi-Do 440-746, Republic of Korea

Supporting Information

ABSTRACT: Recently, silver nanowires (AgNWs) have attracted considerable interest for their potential application in flexible transparent conductive films (TCFs). One challenge for the commercialization of AgNW-based TCFs is the low conductivity and stability caused by the weak adhesion forces between the AgNWs and the substrate. Here, we report a highly bendable, conductive, and transparent AgNW film, which consists of an underlying poly(diallyldimethyl-ammonium chloride) (PDDA) and AgNW composite bottom layer and a top layer-by-layer (LbL) assembled graphene oxide (GO) and PDDA overcoating layer (OCL). We demonstrated that PDDA could increase the adhesion between the AgNW and the substrate to form a uniform AgNW network and could also serve to improve the stability of the GO OCL. Hence, a highly bendable, conductive, and transparent AgNW−PDDA−GO composite TCF on a poly(ethylene terephthalate) (PET) substrate with Rs ≈ 10 Ω/sq and T ≈ 91% could be made by an all-solution processable method at room temperature. In addition, our AgNW−PDDA−GO composite TCF is stable without degradation after exposure to H_2S gas or sonication.

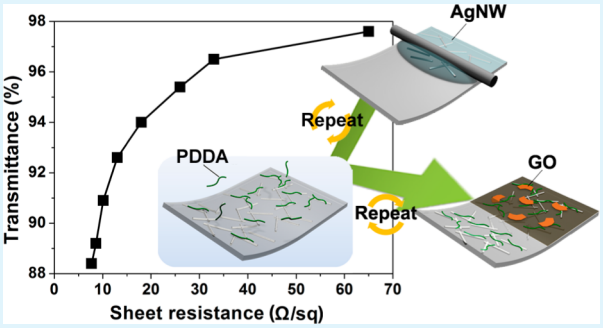

KEYWORDS: *transparent conductors, silver nanowires, materials science, polymers*

INTRODUCTION

Transparent conductive films (TCFs), which provide both good transmittance and electrical conductivity, are key components in optoelectronic devices such as touch screens, photovoltaic cells, liquid crystal displays (LCDs), and light-emitting diodes (LEDs).[1] Today, the most commonly used TCFs in the electronics industry are composed of indium tin oxide (ITO).[2] However, ITO has some inherent shortcomings, including its high brittleness and low adhesion to polymeric materials, which make it unable to meet some requirements of flexible and bendable electronic devices. Another shortcoming is the soaring price of indium metal with the reduction of mineral deposits.[3] Due to the eager demand for alternatives to ITO, many materials, including carbon nanotubes, graphene, conductive polymers, and metal grids, have been investigated.[4−8] However, these materials have their own problems, such as low conductivity/transmittance and low performance with a high manufacturing cost, which hinder their applications.

Recently, silver nanowire (AgNW) has become a promising candidate for replacing ITO due to its excellent electrical, thermal, and optical properties.[9] Through continuous improvement, flexible, transparent, and conductive AgNW films have been achieved using various techniques including transfer printing, air-spraying, and bar coating.[10−14] Despite this exciting achievement, several challenging issues remain, especially the weak adhesion forces between the AgNWs and substrates, which hinder the conductivity and stability of AgNW-based TCFs.[15−17] To solve this problem, inventive methods, such as those using poly(3,4-ethylenedioxythiophene):poly-(styrenesulfonate) (PEDOT:PSS)[15] or reduced graphene oxide (rGO)[16,17] as an overcoating layer (OCL), have been reported. However, since PEDOT:PSS and rGO have strong light absorption, using these materials as the OCL will sacrifice the transmittance of AgNW-based TCFs. Recently, an ultrathin graphene oxide (GO) layer has been reported as an OCL for an AgNW TCF.[18,19] The GO sheets adhere to the O_2 plasma-treated poly(ethylene terephthalate) (PET) substrate through hydrophilic−hydrophilic interaction to improve the mechanical stability and conductivity of the AgNW film. Although GO is known as an insulator, the ultrathin thickness of the GO layer allows a direct tunneling current through a nanometer thickness without decreasing the conductivity of the AgNW film.[18] However, the interaction between the GO and the PET gradually weakens over time due to the molecular rearrangement of the PET surface,[20] thereby hindering the stability of the GO OCL.

Poly(diallyldimethylammonium chloride) (PDDA) shows good affinity to various materials and can form self-assembled monolayers on the surfaces of quartz, glass, metals, and polymers.[21] In addition, PDDA is a polycationic polymer that

Received: July 1, 2013
Accepted: August 22, 2013
Published: August 22, 2013

   dx.doi.org/10.1021/am402578d | ACS Appl. Mater. Interfaces 2013, 5, 9155−9160

can be assembled with negatively charged Ag nanoparticles,[22] AgNWs,[23] and GO sheets[21] to form stable composite films. In this work, we demonstrate that PDDA can increase the adhesion between the AgNWs and the substrate and can improve the stability of the GO OCL. Due to the introduction of PDDA, a highly bendable, conductive, and transparent AgNW−PDDA−GO TCF on a PET substrate with Rs ≈ 10 Ω/sq and T ≈ 91% can be fabricated through an all-solution processable and low-cost method.

EXPERIMENTAL SECTION

Materials. The PDDA (M_w 100 000−200 000), bis-(trifluoromethane)sulfonimide lithium salt (TFSI Li), and polyethylenimine (PEI) (M_w 25 000) were purchased from Sigma-Aldrich (Korea). The AgNW dispersion was purchased from Aiden (Korea). The mean length and diameter of the nanowires were 20 μm and 45 nm, respectively. Before use, the AgNW dispersion was centrifuged and redispersed in isopropyl alcohol (IPA) to remove any residual ligand (poly(vinylpyrrolidone) (PVP)) in the solution. GO nano sheets were prepared using a modified Hummers method.[24] Deionized (DI) water (18 MΩ·cm, Pure Up90) was used in the preparation of the samples and polymer solutions.

Treatment of the PET. The PET films were first cleaned with EtOH and DI water and dried with N_2 gas flow. Then, the PET films were treated with O_2 plasma and subsequently immersed in a PDDA solution (1 mg/mL). After 5 min, the PET films were washed with DI water and dried with N_2 gas flow. In this way, the surfaces of the PET films were modified with PDDA.

Fabrication of the AgNW−PDDA−GO Composite TCF. The method used to fabricate the highly bendable, conductive, and transparent AgNW−PDDA−GO composite film on the PET, which consists of an underlying PDDA and AgNW composite bottom layer and a top layer-by-layer (LbL) assembled PDDA and GO OCL, is schematically illustrated in Figure 1a. The whole experiment was

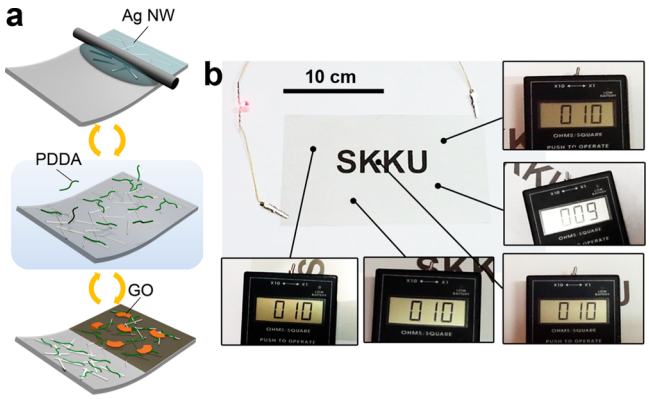

Figure 1. (a) Schematic illustration of the fabrication procedure for preparing AgNW−PDDA−GO composite TCF. (b) A photograph of AgNW−PDDA−GO composite TCF on PET substrate (100 mm × 200 mm). Insets present the sheet resistance of the film at different places.

conducted in an ambient environment (25 °C, 40% relative humidity), and no heating or pressing process was used. First, the AgNW, which was dispersed in an IPA solution (0.5 mg/mL), was applied on the PDDA-modified PET film by a machine-controlled wire-wound rod (Meyer rod 10#, where the speed was set to 40 mm/s). After evaporation of the IPA for 3 min, the film was immersed in a PDDA solution (1 mg/mL) for 5 min, followed by an extensive DI water rinse and N_2 gas blow-drying. These two steps were repeated to make an (AgNW/PDDA)*n (n represents the number of repetitions) bottom layer. Next, the GO solution (0.5 mg/mL) was carefully casted onto the film. After 5 min, the GO solution was removed and the resulting film was rinsed with DI water. Then, the film was immersed in a PDDA solution (1 mg/mL) for 5 min and then rinsed with DI water. After repeating these two steps several times, a (GO/PDDA)*m (m represents the number of repetitions) OCL was fabricated. Through this simple, all-solution processable, and low-cost method, a large scale AgNW−PDDA−GO composite TCF on a PET substrate with Rs ≈ 10 Ω/sq and T ≈ 91% was obtained (Figure 1b).

Counter Ion Exchange. To exchange Cl^- with bis-(trifluoromethanesulfonyl)imide ($TFSI^-$), the (GO/PDDA)*4/(AgNW/PDDA)*7 film was immersed in a bis(trifluoromethane)-sulfonimide lithium salt solution (2 mg/mL) for 10 min. Then, the sample was washed with DI water and dried with N_2 gas flow.

Characterization. The morphologies of the samples were characterized by scanning electron microscopy (SEM) (JEOL JSM-7600F and XL30 ESEM FEG), atomic force microscopy (AFM) (SPI3800N, SII), and optical microscopy (OM) (Olympus BX51, Microscopes Inc.). X-ray photoelectron spectroscopy (XPS) measurements were performed in a SIGMA PROBE (ThermoVG, UK) using a monochromatic Al−K X-ray source at 100 W. The sheet resistance values were measured with a Keithley 4200 semiconductor characterization system. The transmittance was measured using a Shimadzu 1650PC.

RESULTS AND DISCUSSION

The conductivity of the (AgNW/PDDA)*n bottom layer can be easily controlled by adjusting the deposition cycles. The variations of the sheet resistance and transmittance of the (AgNW/PDDA)*n film during the fabrication process are shown in Figure 2. The transmittance of the (AgNW/

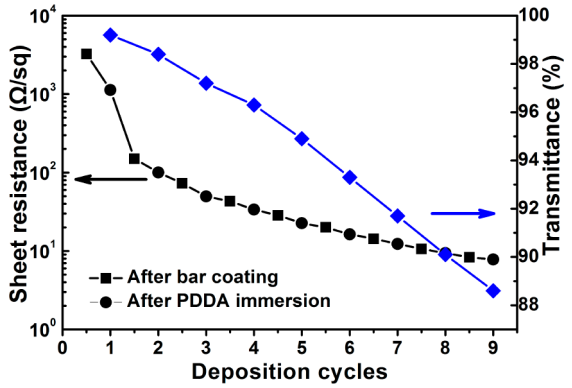

Figure 2. Transmittance and sheet resistance of (AgNW/PDDA)*n film after bar coating AgNW (■) and PDDA immersion (●).

PDDA)*n film decreased linearly during the fabrication process, indicating an even increase in the density of the AgNW network. We used the method reported by Peter Peumans et al.[10] to calculate the coverage of AgNWs on (AgNW/PDDA)*n films. According to the top-view SEM images (Figure S1, Supporting Information), the coverage of the AgNWs on the (AgNW/PDDA)*n (n = 2, 4, 6, and 8) films were 7.1%, 13.9%, 22.3%, and 28.7%, respectively. By increasing the number of deposition cycles, we could fabricate a highly conductive and transparent (AgNW/PDDA)*7 film with Rs = 12.3 Ω/sq and T = 91.7%. Even though the film was not protected by an OCL, it could withstand folding and rolling over a toothpick (D = 1.9 mm) without disconnection (supplemental movie, Supporting Information).

PDDA plays an important role in the film fabrication process. We noticed that direct deposition of the AgNWs onto the O_2 plasma-treated PET substrate without any PDDA modification caused strong aggregation of the AgNWs (Figure 3a). This

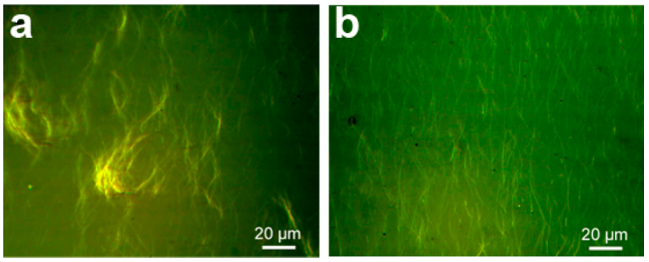

Figure 3. OM images of AgNWs applied by bar coating on O_2 plasma-treated PET substrate without (a) and with (b) PDDA modification.

uneven distribution of AgNWs, which was caused by the coffee ring effect,[25] would lead to a significant loss of conductivity. In this case, by applying the AgNWs repeatedly, we could only obtain an AgNW film with Rs = ~184 Ω/sq and T = 88% (Figure S2, Supporting Information). In contrast, on the PDDA-modified PET substrate, which had same wettability as the O_2 plasma-treated substrate (Figure S3, Supporting Information), an even distribution of AgNWs was observed (Figure 3b). It is known that PVP-coated AgNWs are negatively charged,[23] which is attributed to the presence of the negatively charged hydroxo- and oxo-groups on the AgNW surface, which are generated by the oxidation of the silver.[26] Therefore, once the AgNW solution was applied, the AgNWs were anchored by the strong electrostatic interactions with the positively charged PDDA modified on the substrate, reducing the aggregation caused by the coffee ring effect during the solvent evaporation. This uniform AgNW network is favorable for the fabrication of highly transparent and conductive AgNW films with small variations in the surface resistivity.

It is noteworthy that, after the bar coating of the AgNWs, immersion in the PDDA solution for 5 min would lead to better conductivity of the (AgNW/PDDA)*n film. In the first deposition cycle, for example, the sheet resistance decreased from 3240 to 1130 Ω/sq after the PDDA immersion. Meanwhile, immersion of the AgNW film into a PDDA solution did not decrease its transmittance (Figure S4, Supporting Information). As a comparison, immersion of the as-prepared AgNW film into DI water or an NaCl aqueous solution does not significantly increase the conductivity. Since AgNWs were the only conductive material on the PET substrate, the conductivity enhancement indicated that new conducting paths were formed during the PDDA immersion. The adhesion between the AgNWs and the substrate was also greatly enhanced after the PDDA immersion. The AgNW–PDDA composite film could survive a Scotch tape test, while an AgNW film without the PDDA immersion steps was removed completely by peeling off the tape (Figure S5, Supporting Information). Increasing the adhesion between the AgNWs and the substrate could prevent the detachment of the AgNWs during the fabrication process, which is crucial for the formation of a uniform AgNW network over a large area.

To understand the role of PDDA in the conductivity and adhesion enhancement, we used SEM to characterize the morphologies of the AgNWs before and after the PDDA immersion. Due to the weak adhesion forces between the AgNWs and the substrates, some AgNWs stood up on the substrate after the bar coating process, making poor contact between nanowires (Figure 4a). After the PDDA immersion, the AgNWs were laid down on one another and generated new conducting paths (Figure 4b). XPS was used to characterize the

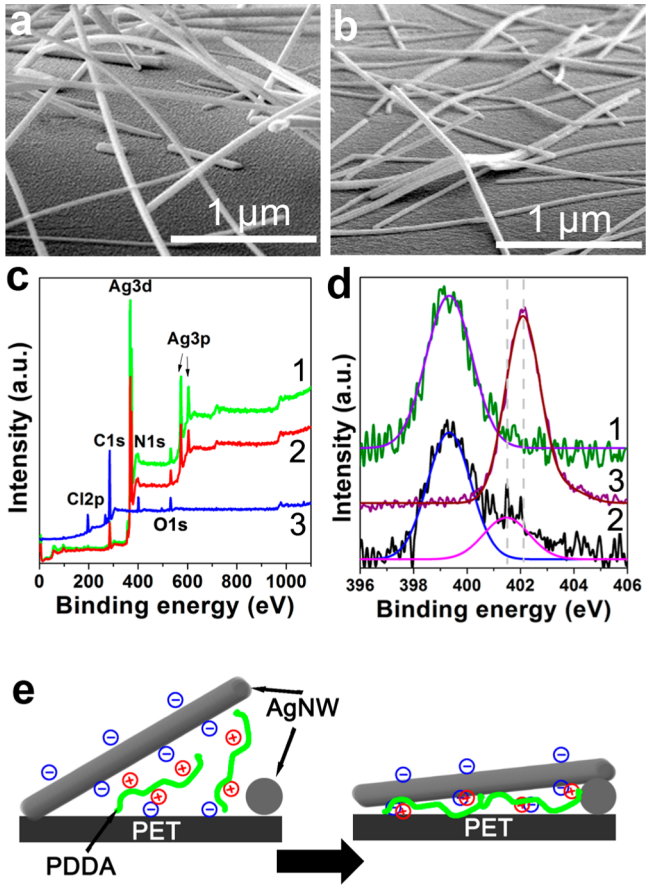

Figure 4. Tilt-view SEM images of AgNWs on PET substrate before (a) and after (b) immersion in PDDA solution. XPS survey (c) and the high-resolution N1s spectra (d) for AgNWs before (spectra 1) and after the PDDA immersion (spectra 2). Also included are the corresponding spectra for PDDA as a reference (spectra 3). (e) Schematic illustration of PDDA bonding to negatively charged groups of AgNWs and the substrate through electrostatic interaction.

surface chemical composition of the AgNW film before and after the PDDA immersion. In Figure 4c,d, the XPS survey spectra of the as-prepared AgNW film revealed an N1s single peak at 399.3 eV, which corresponds to the N atom of the residual PVP on the AgNWs.[27] After the PDDA immersion, a new N1s peak emerged at 401.5 eV, which corresponds to the N of the PDDA.[28] Compared to the N1s peak for pure PDDA on the substrate, the PDDA N1s peak for the AgNW–PDDA composite film shifted negatively by ~0.6 eV, which was caused by a charge transfer from the negatively charged hydroxo- and oxo-groups on the AgNW to the positively charged N atom of the PDDA,[28] indicating the formation of ionic bonds between the AgNW and PDDA.

On the basis of the above results, we believe that the flattening of the AgNW network from 3D to 2D was attributed to the strong electrostatic interaction between the PDDA, AgNWs, and PET. As schematically shown in Figure 4e, it is suggested that ionic bonds should be formed between the positively charged quaternary ammonium group on the PDDA and the negatively charged groups of the AgNWs and PET substrate,[29,30] allowing a tight bond of the AgNWs to the substrate and consolidation of the contact between AgNWs, leading to enhanced adhesion and conductivity. The negatively charged groups on the PET are derived from the O_2 plasma. Previously, a mechanical pressing method was reported to

enhance the conductivity of an AgNW TCF by flattening the AgNWs.[31] However, the mechanical pressing process is not suitable for fragile substrates or delicate devices. Hence, an all-solution processable and pressing-free method is needed in order to fabricate the AgNW TCF. In addition to flattening the AgNW network, the PDDA could also enhance the adhesion between the AgNWs and the substrate and decrease the aggregation of the AgNWs caused by the coffee ring effect, thereby increasing the stability, conductivity, and transmittance at the same time. Therefore, we strongly believe that our method, which uses PDDA to enhance the adhesion of the AgNWs, is much better than the mechanical pressing method for enhancing the conductivity of an AgNW TCF without deforming or damaging the substrate. On the other hand, another polycation polymer, PEI, could also enhance the conductivity and adhesion of the AgNW film. However, the enhanced conductivity of the AgNW/PEI composite film decreases in an alkaline solution (pH > 10) because the amino group loses its positive charge at the high pH.[32] Therefore, the PDDA, which has permanently positively charged quaternary amine groups, is a suitable candidate for enhancing the adhesion of AgNWs.

The LbL technique is an efficient method for controlling the thickness of the resultant film.[33−39] Hence, we used the LbL technique to fabricate a GO/PDDA OCL. The changes in the sheet resistance, transmittance and surface wettability of the (AgNW/PDDA)*7 film while fabricating the (GO/PDDA)*m OCL are shown in Table 1. The sheet resistance decreased with

Table 1. Dependence of Sheet Resistance, Transmittance, and Contact Angle (CA) of (GO/PDDA)*m/(AgNW/PDDA)*7 Film and Thickness of (GO/PDDA)*m Film (H) on the Number of Cycles of (GO/PDDA)*m Film

	m					
	0	1	2	3	4	5
Rs (Ω/sq)	12.3	12.1	11.5	10.9	10.1	10.6
$T_{\lambda=550}$	91.7	91.6	91.4	91.1	90.9	90.6
CA (°)	80	63	44	31	25	25
H (nm)	0	2.1	3.9	6.2	8.1	10.3

an increasing number of deposition cycles of the (GO/PDDA)*m, which was caused by the GO sheets pressing upon the AgNWs and further consolidating their contacts.[18,19] The sheet resistance of the (GO/PDDA)*m/(AgNW/PDDA)*7 film reached the minimum at m = 4, and further increases in the number of deposition cycles led to a rise in the sheet resistance, since the tunneling current decreased with the increase of the (GO/PDDA)*m thickness. Therefore, in this work, we chose (GO/PDDA)*4 as the OCL.

The inset in Figure 5 reveals the thin (GO/PDDA)*4 film covered on the AgNWs, firmly pressing the AgNWs to the substrate. According to the AFM, the thickness of the (GO/PDDA)*4 film was ∼8 nm (Table 1). From the AFM images (Figure S6, Supporting Information), the root-mean-square (RMS) roughness of the (AgNW/PDDA)*7 film was 35.8 nm. For the (GO/PDDA)*4/(AgNW/PDDA)*7 film, in which the AgNWs were covered with a rigid GO/PDDA OCL, the RMS roughness was reduced to 18.6 nm, which is half of that of the (AgNW/PDDA)*7 film. Figure 5 presents the conductivity and transmittance of the (GO/PDDA)*4/(AgNW/PDDA)*n films. In terms of the conductivity and transmittance, the (GO/PDDA)*4/(AgNW/PDDA)*7 film showed the best

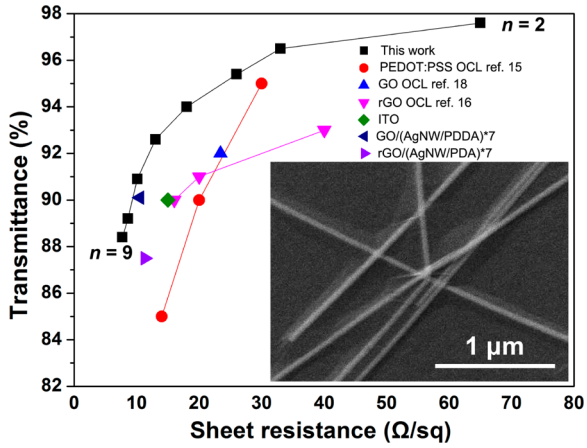

Figure 5. Plot of T (550 nm) vs Rs for (GO/PDDA)*4/(AgNW/PDDA)*n film (n = 2−9), GO/(AgNW/PDDA)*7, and rGO/(AgNW/PDDA)*7. The data for the other AgNW films were taken from literature and replotted for comparison. Inset: Top-view SEM of (GO/PDDA)*4 OCL covered on AgNWs.

performance, with Rs = ∼10 Ω/sq and T = ∼91%, which are superior to the values obtained using the commercialized ITO on PET.[2] Since PDDA and GO have low absorption in the visible light region, the ultrathin (GO/PDDA)*4 film, when used as an OCL, would only cause a 1% decrease in the transmittance (Figure S7, Supporting Information), which is much lower than the transmittances of other OCLs fabricated by using rGO[16,17] or PEDOT:PSS.[15] As a comparison, GO and rGO OCL with an 8 nm thickness would cause 1.6% and 4.2% decreases, respectively, in the transmittance of the (AgNW/PDDA)*7 film (Figure 5). Hence, since PDDA could reduce the aggregation caused by the coffee ring effect and (GO/PDDA)*4 OCL had less light absorption, (GO/PDDA)*4/(AgNW/PDDA)*n films exhibited better performance than the GO/AgNW film and AgNW films with rGO or PEDOT:PSS OCL fabricated by the spray coating or spin coating method (Figure 5).

Counter ions of the PDDA in (GO/PDDA)*4/(AgNW/PDDA)*n films may influence the performance when used in devices such as solar cells.[40] This problem can be easily solved by ion exchange.[41] To exchange Cl^- with $TFSI^-$, which was reported to have the best performance in solar cells,[40] the (GO/PDDA)*4/(AgNW/PDDA)*7 film was immersed in a bis(trifluoromethane)sulfonimide lithium salt solution for 10 min. After the ion exchange (Figure S8, Supporting Information), the signal of fluorine that is associated with $TFSI^-$ was detected at 688.7 eV and the signal of chlorine vanished, indicating that the Cl^- anions in the (GO/PDDA)*4/(AgNW/PDDA)*7 film were exchanged with $TFSI^-$ anions. In addition, the ion exchange process did not influence the conductivity of the (GO/PDDA)*4/(AgNW/PDDA)*7 film.

The stability of AgNW TCFs is one of the most crucial issues for their potential applications. Since the (GO/PDDA)*4 OCL firmly pressed the AgNWs to the substrate, the stability of the AgNW-based electrodes was greatly enhanced. As shown in Figure 6a, we hardly observed any appreciable change in the conductivity of the (GO/PDDA)*4/(AgNW/PDDA)*7 films after 2 months or after immersion in EtOH and DI water for 9 h. On the contrary, mainly due to a weak adhesion force between the AgNWs and the substrate, the sheet resistance of

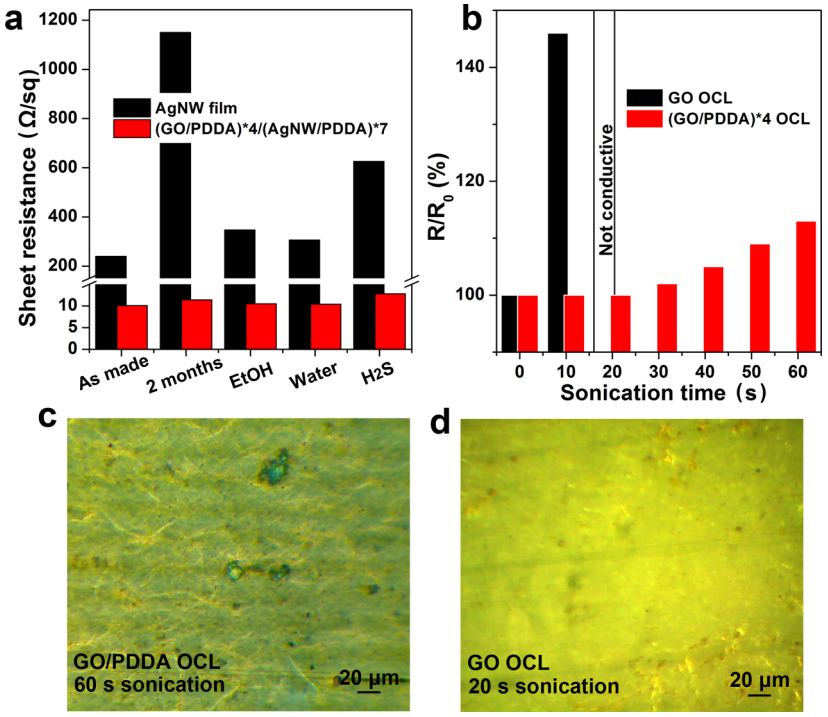

Figure 6. (a) Stability of (GO/PDDA)*4/(AgNW/PDDA)*7 and AgNW films. (b) Change of sheet resistance of (AgNW/PDDA)*7 films with GO (black) and (GO/PDDA)*4 OCL during sonication. OM images of (c) (GO/PDDA)*4/(AgNW/PDDA)*7 after sonication for 60 s and (d) (AgNW/PDDA)*7 with GO OCL after sonication for 20 s.

the pure AgNW film increased 8-fold after 2 months and about 1- and 1.5-fold after immersion in EtOH and DI water for 9 h. Also, (GO/PDDA)*4 could serve as a gas barrier to prevent AgNWs from the oxidation caused by H_2S gas. After exposure to 100 ppm H_2S gas for 1 h, the sheet resistance of the (GO/PDDA)*4/(AgNW/PDDA)*7 film barely increased 3 Ω/sq, but that of the pure AgNW film increased about 3-fold. Bending tests were also performed to test the bendability of the (GO/PDDA)*4/(AgNW/PDDA)*7 film (Figure S9, Supporting Information). The bending test with a bend radius of 0.5 cm was automatically performed by a bending machine, and after 10 000 bending cycles, the sheet resistance of the (GO/PDDA)*4/(AgNW/PDDA)*7 film increased only 1 Ω/sq. For the detachment test, a Scotch tape test was performed. After peeling off the tape from the (GO/PDDA)*4/(AgNW/PDDA)*7 film, the sheet resistance was not changed, indicating that the AgNW/PDDA down layer was well protected by the GO/PDDA OCL (Figure S10, Supporting Information).

More importantly, PDDA greatly increased the stability of the GO OCL. (AgNW/PDDA)*7 films covered with an ∼8 nm GO OCL that was fabricated by spray coating and (GO/PDDA)*4 were immersed in a sonication bath (Powersonic 420, 700 w, work at low power mode), and the sheet resistances of the samples were measured every 10 s. As shown in Figure 6b, the (GO/PDDA)*4/(AgNW/PDDA)*7 film only had a 13% increase in the sheet resistance after sonication in water for 60 s. The strong electrostatic interaction between the PDDA and the GO prevented the OCL from cracking and dispersing during the sonication. Thus, the AgNW network underneath the (GO/PDDA)*4 was well maintained (Figure 6c). On the contrary, the (AgNW/PDDA)*7 that was covered with an ∼8 nm GO OCL was completely removed after sonication for 20 s (Figure 6d).

CONCLUSIONS

In conclusion, we demonstrated a highly bendable, conductive, and transparent AgNW TCF, which consisted of an underlying AgNW/PDDA bottom layer and a top LbL assembled GO/PDDA OCL. Through electrostatic interactions with the AgNWs, PDDA could prevent the aggregation of the AgNWs and increase their adhesion. Also, the LbL assembled GO/PDDA OCL exhibited better stability than the GO OCL and preserved the transmittance better than the PEDOT:PSS and rGO OCLs. Hence, a highly bendable, conductive, and transparent AgNW−PDDA−GO composite TCF on a PET substrate was made by an all-solution processable method at room temperature, exhibiting excellent performance with a sheet resistance of ∼10 Ω/sq and a transmittance of ∼91% and high stability without degradation after exposure to H_2S gas or sonication. Since the solution-based processes are simple and nontoxic materials and inexpensive equipment are used, our new method could play a role in fueling the commercialization of highly bendable, conductive, and transparent AgNW TCFs.

ASSOCIATED CONTENT

Supporting Information

Ten additional figures and a movie showing the conductive and transparent film. This material is available free of charge via the Internet at http://pubs.acs.org.

AUTHOR INFORMATION

Corresponding Author

*Tel: +82-31-290-4566. Fax: +82-31-290-5924. E-mail: hyoyoung@skku.edu.

Notes

The authors declare no competing financial interest.

■ ACKNOWLEDGMENTS

This work was supported by the National Research Foundation of Korea (NRF) grant funded by the Korea government (MSIP) (Grant No. 2006-0050684). The authors would like to acknowledge Shanshan Chen (JLU) for SEM and QCM measurements and Sae Mi Lee (SKKU) for kindly offering GO.

■ ABBREVIATIONS

AgNW, silver nanowire
PDDA, poly(diallyldimethyl-ammonium chloride)
LbL, layer-by-layer
OCL, overcoating layer
TCF, transparent conductive film
PEI, polyethylenimine
$TFSI^-$, bis(trifluoromethane)sulfonamide

■ REFERENCES

(1) Gordon, R. G. *MRS Bull.* **2000**, *25*, 52−57.
(2) Lewis, B. G.; Paine, D. C. *MRS Bull.* **2000**, *25*, 22−27.
(3) Leterrier, Y.; Médico, L.; Demarco, F.; Månson, J. A. E.; Betz, U.; Escolà, M. F.; Olsson, M. K.; Atamny, F. *Thin Solid Films* **2004**, *460*, 156−166.
(4) Wu, Z.; Chen, Z.; Du, X.; Logan, J. M.; Sippel, J.; Nikolou, M.; Kamaras, K.; Reynolds, J. R.; Tanner, D. B.; Hebard, A. F.; Rinzler, A. G. *Science* **2004**, *305*, 1273−1276.
(5) Tvingstedt, K.; Inganäs, O. *Adv. Mater.* **2007**, *19*, 2893−2897.
(6) Carroll, D. L.; Czerw, R.; Webster, S. *Synth. Met.* **2005**, *155*, 694−697.
(7) Sukang, B.; Kim, H.; Lee, Y.; Xu, X.; Park, J.; Zheng, Y.; Balakrishnan, J.; Lei, T.; Kim, H. R.; Song, Y. I.; Kim, Y.; Kim, K. S.; Özyilmaz, B.; Ahn, J.; Hong, B. H.; Iijima, S. *Nat. Nanotechnol.* **2010**, *5*, 574−578.
(8) Gruner, G. *J. Mater. Chem.* **2006**, *16*, 3533−3539.
(9) Lee, J.-Y.; Connor, S. T.; Cui, Y.; Peumans, P. *Nano Lett.* **2008**, *8*, 689−692.
(10) Gaynor, W.; Burkhard, G. F.; McGehee, M. D.; Peumans, P. *Adv. Mater.* **2011**, *23*, 2905−2910.
(11) Madaria, A. R; Kumar, A.; Zhou, C. *Nanotechnology* **2011**, *22*, 245201−245208.
(12) Hu, L.; Kim, H. S.; Lee, J-Y; Peumans, P.; Cui, Y. *ACS Nano* **2010**, *4*, 2955−2963.
(13) Xu, F.; Durham, J. W., III; Wiley, B. J.; Zhu, Y. *ACS Nano* **2011**, *5*, 1556−1563.
(14) Scardaci, V.; Coull, R.; Lyons, P. E.; Rickard, D.; Coleman, J. N. *Small* **2011**, *7*, 2621−2628.
(15) Choi, D. Y; Kang, H. W.; Sung, H. J.; Kim, S. S. *Nanoscale* **2013**, *5*, 977−983.
(16) Ahn, Y.; Jeong, Y.; Lee, Y. *ACS Appl. Mater. Interfaces* **2012**, *4*, 6410−6414.
(17) Kholmanov, I. N.; Stoller, M. D.; Edgeworth, J.; Lee, W. H.; Li, H.; Lee, J.; Barnhart, C.; Potts, J. R.; Piner, R.; Akinwande, D.; Barrick, J. E.; Ruoff, R. S. *ACS Nano* **2012**, *6*, 5157−5163.
(18) Moon, I. K.; Kim, J. I.; Lee, H.; Hur, K.; Kim, W. C.; Lee, H. *Sci. Rep.* **2013**, *3*, 1112.
(19) Zhang, X.; Wong, W. N. M.; Yuen, M. M. F. 12th IEEE International Conference on Nanotechnology (IEEE-NANO), Birmingham, United Kingdom, Aug 20−23, 2012; DOI: 10.1109/NANO.2012.6322001.
(20) Li, J.; Oh, K.; Yu, H. *Chin. J. Polym. Sci.* **2005**, *23*, 187−196.
(21) Kotov, N. A.; Dékány, I.; Fendler, J. H. *Adv. Mater.* **1996**, *8*, 637−641.
(22) Kvítek, L.; Panáček, A.; Soukupová, J.; Kolář, M.; Večeřová, R.; Prucek, R.; Holecová, M.; Zbořil, R. *J. Phys. Chem. C* **2008**, *112*, 5825−5834.
(23) Luu, Q. N.; Doorn, J. M.; Berry, M. T.; Jiang, C.; Lin, C.; May, P. S. *J. Colloid Interface Sci.* **2011**, *356*, 151−158.
(24) Stankovich, S.; Dikin, D. A.; Dommett, G. H. B.; Kohlhaas, K. M.; Zimney, E. J.; Stach, E. A.; Piner, R. D.; Nguyen, S. T.; Ruoff, R. S. *Nature* **2006**, *442*, 282−286.
(25) Deegan, R. D.; Bakajin, O.; Dupont, T. F.; Huber, G.; Nagel, S. R.; Witten, T. A. *Nature* **1997**, *389*, 827−829.
(26) Levard, C.; Hotze, E. M.; Lowry, G. V.; Brown, G. E., Jr. *Environ. Sci. Technol.* **2012**, *46*, 6900−6914.
(27) Jiang, P.; Li, S.-Y.; Xie, S.-S.; Gao, Y.; Song, L. *Chem.—Eur. J.* **2004**, *10*, 4817−4821.
(28) Wang, S.; Yu, D.; Dai, L. *J. Am. Chem. Soc.* **2011**, *133*, 5182−5185.
(29) Ren, W.; Fang, Y.; Wang, E. *ACS Nano* **2011**, *5*, 6425−6433.
(30) Zhang, X.; Fujishima, A.; Jin, M.; Emeline, A. V.; Murakami, T. *J. Phys. Chem. B* **2006**, *110*, 25142−25148.
(31) Tokuno, T.; Nogi, M.; Karakawa, M.; Jiu, J.; Nge, T. T.; Aso, Y.; Suganuma, K. *Nano Res.* **2011**, *4*, 1215−1222.
(32) Griffith, A.; Notley, S. M. *J. Colloid Interface Sci.* **2012**, *369*, 210−215.
(33) Decher, G. *Science* **1997**, *277*, 1232−1237.
(34) Hammond, P. T. *Adv. Mater.* **2004**, *16*, 1271−1293.
(35) Zhang, X.; Chen, H.; Zhang, H. *Chem. Commun.* **2007**, 1395−1405.
(36) Podsiadlo, P.; Shim, B. S.; Kotov, N. A. *Coord. Chem. Rev.* **2009**, *253*, 2835−2851.
(37) Such, G. K.; Johnston, A. P. R.; Caruso, F. *Chem. Soc. Rev.* **2011**, *40*, 19−29.
(38) Jiang, G.; Baba, A.; Ikarashi, H.; Xu, R.; Locklin, J.; Khan, K. R.; Shinbo, K.; Kato, K.; Kaneko, F.; Advincula, R. *J. Phys. Chem. C* **2007**, *111*, 18687−18694.
(39) Schlenoff, J. B. *Langmuir* **2009**, *25*, 14007−14010.
(40) Xia, J.; Masaki, N.; Lira-Cantu, M.; Kim, Y.; Jiang, K.; Yanagida, S. *J. Am. Chem. Soc.* **2008**, *130*, 1258−1263.
(41) Wang, L.; Lin, Y.; Peng, B.; Su, Z. *Chem. Commun.* **2008**, 5972−5975.